Supplement of Atmos. Chem. Phys., 25, 18249–18265, 2025
https://doi.org/10.5194/acp-25-18249-2025-supplement

Atmospheric Chemistry and Physics
Open Access
EGU

Supplement of

Volume uptake of carbonyls during diffusional ice crystal growth

Jackson Seymore et al.

Correspondence to: Jackson Seymore (seymorej@uni-mainz.de)

Equation S1. Sonntag Parameterization

$$\log e_i = -6024.5282 / T + 24.721994 + 1.0613868\,10^{-2} \cdot T - 1.3198825\,10^{-5} \cdot T^2 - 0.49382577 \cdot \log T \quad \text{(S1)}$$

where the air temperature (T) is in units of K and saturation pressure of water vapor over ice (e_i) is in units of hPa.

Table S1. Bubbler Concentrations and Henry Solubilities

	H^{cp}		**$H_s{}^{cp}T$**	**Target Flowtube Gas Concentration**	**Molar Mass**	**Target Bubbler Liquid concentration (uM)**		
	mol/(m^3 Pa)	M/atm	K	ppbv	g/mol	-40 ºC (d =165)	-30 ºC (d = 55)	-20 ºC (d = 18)
Benzaldehyde	0.4	40.53	5200	10	106.12	109	36	12
MVK	0.26	26.34	7800	10	70.09	91	30	10
Methacrolein	0.045	4.56	4600	10	70.09	12	4	1
Acetaldehyde	0.13	13.17	5900	10	44.05	38	13	4
Formaldehyde	32	3242.4	7100	10	30.03	10447	3482	1159
Acetone	0.27	27.36	5500	10	58.08	76	25	8
Nopinone	14	1418.55		10	138.21	2341	780	260
Norcamphor	0.43	43.57	5100	10	110.15	116	39	13
Camphor	0.54	54.72	4800	10	152.23	142	47	16
Diacetyl	0.73	73.97	5700	10	86.09	209	70	23
Glyoxal	4100	415433	7500	10	58.04	1389975	463325	154161
Hydroxyacetone	77	7802.03		10	74.08	12873	4291	1428
Methylglyoxal	35	3546.38	7500	10	72.06	11866	3955	1316
Propionaldehyde	0.099	10.03	4300	10	58.08	25	8	3

Table S2. Target m/z for MS analysis (Compounds given in elution order)

Species	Elemental Formula	Monoisotopic Mass (Da)	MS Analyte	Analyte Elemental Formula	Target m/z used $[M-H]^-$	Expected RT (min)
Hydroxyacetone	C3H6O2	74.0368	Hydroxyacetone-DNPH	C9H10N4O5	253.0573	1.3
Formaldehyde	CH2O	30.0106	Formaldehyde-DNPH	C7H6N4O4	209.0311	1.9
Acetaldehyde	C2H4O	44.0262	Acetaldehyde-DNPH	C8H8N4O4	223.0467	2.7
Acetone	C3H6O	58.0419	Acetone-DNPH	C9H10N4O4	237.0624	3.5
Propionaldehyde	C3H6O	58.0419	Propionaldehyde-DNPH	C9H10N4O4	237.0624	3.9
Methacrolein	C4H6O	70.0419	Methacrolein-DNPH	C10H10N4O4	249.0624	4.5
MVK	C4H6O	70.0419	MVK-DNPH	C10H10N4O4	249.0624	4.8
Benzaldehyde	C7H6O	106.0419	Benzaldehyde-DNPH	C13H10N4O4	285.0624	5.4
Glyoxal	C2H2O2	58.0055	Glyoxal-bis-DNPH	C14H10N8O8	417.0534	5.7
Norcamphor	C7H10O	110.0732	Norcamphor-DNPH	C13H14N4O4	289.0937	5.7
Methylglyoxal	C3H4O2	72.0211	Methylglyoxal-bis-DNPH	C15H12N8O8	431.0700	6.5
Diacetyl	C4H6O2	86.0368	Diacetyl-bis-DNPH	C16H14N8O8	445.0856	7.2
Nopinone	C9H14O	138.1045	Nopinone-DNPH	C15H18N4O4	317.1250	7.8
Camphor	C10H16O	152.1201	Camphor-DNPH	C16H20N4O4	331.1412	8.2

Table S3. Ice uptake Coefficients converted to mol m^{-3} Pa^{-1}

	***K* at –20 ºC**	***K* at –30 ºC**	***K* at –40 ºC**
MVK	$(1.05 \pm 0.59) \times 10^{-5}$	$(1.02 \pm 1.03) \times 10^{-6}$	$(4.65 \pm 4.26) \times 10^{-6}$
Acetaldehyde	$(6.02 \pm 1.67) \times 10^{-5}$	$(4.82 \pm 6.79) \times 10^{-4}$	$(1.60 \pm 0.84) \times 10^{-3}$
Acetone	$(8.88 \pm 2.55) \times 10^{-5}$	$(1.45 \pm 1.90) \times 10^{-4}$	$(1.11 \pm 1.22) \times 10^{-3}$
Benzaldehyde	$(3.65 \pm 1.36) \times 10^{-8}$	$(3.28 \pm 2.46) \times 10^{-7}$	$(7.38 \pm 5.87) \times 10^{-6}$
Camphor	$(2.41 \pm 0.33) \times 10^{-7}$	$(3.46 \pm 3.79) \times 10^{-6}$	$(3.08 \pm 2.19) \times 10^{-5}$
Diacetyl	$(1.75 \pm 0.54) \times 10^{-6}$	$(1.57 \pm 1.45) \times 10^{-5}$	$(6.86 \pm 5.70) \times 10^{-4}$
Formaldehyde	$(9.96 \pm 2.93) \times 10^{-5}$	$(6.83 \pm 9.78) \times 10^{-3}$	$(5.33 \pm 3.26) \times 10^{-2}$
Glyoxal	$(4.28 \pm 0.58) \times 10^{-6}$	$(3.35 \pm 1.21) \times 10^{-5}$	$(5.39 \pm 7.96) \times 10^{-4}$
Hydroxyacetone	$(7.77 \pm 1.08) \times 10^{-7}$	$(1.16 \pm 1.55) \times 10^{-5}$	$(1.83 \pm 2.39) \times 10^{-4}$

Methacrolein	$(1.87 \pm 0.90) \times 10^{-6}$	$(5.69 \pm 7.06) \times 10^{-6}$	$(1.09 \pm 1.58) \times 10^{-4}$
Methylglyoxal	$(3.47 \pm 1.42) \times 10^{-6}$	$(2.77 \pm 1.81) \times 10^{-5}$	$(2.04 \pm 1.75) \times 10^{-4}$
Nopinone	$(4.41 \pm 1.14) \times 10^{-9}$	$(5.44 \pm 3.30) \times 10^{-8}$	$(0.85 \pm 1.26) \times 10^{-6}$
Norcamphor	$(2.05 \pm 0.98) \times 10^{-8}$	$(4.48 \pm 1.35) \times 10^{-8}$	$(3.17 \pm 3.91) \times 10^{-6}$
Propionaldehyde	$(6.54 \pm 5.94) \times 10^{-5}$	$(1.04 \pm 1.14) \times 10^{-4}$	$(1.51 \pm 1.66) \times 10^{-3}$

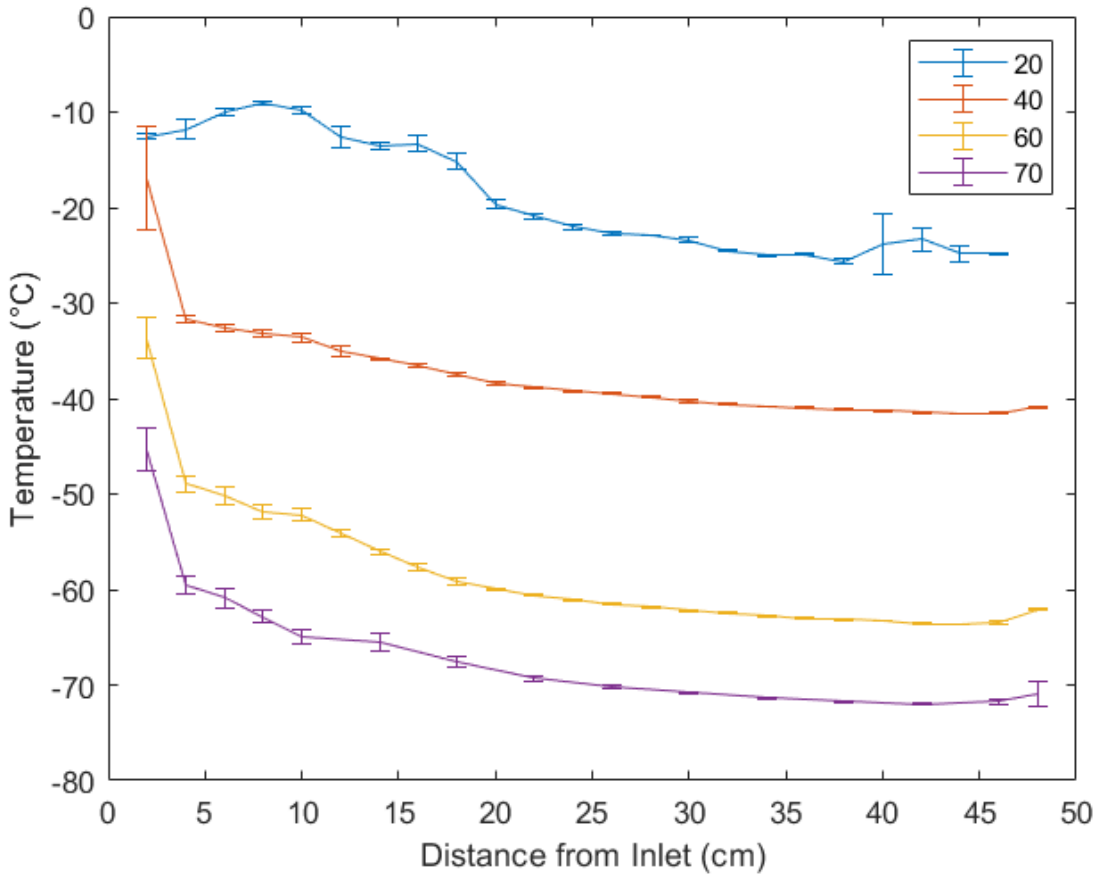

Figure S1. Temperature Profile along z-axis of Flowtube

Section S1. Discussion on Entropy-Enthalpy Compensation

Reviewing this data in accordance with the definitions laid out by Liu and Guo, (2001) and Pan et al. (2015), it appears unlikely that the Entropy-Enthalpy Compensation (EEC) effect seen here is a spurious finding. The linearity from the regressions in Table 3 are strong and thus there is relatively low standard error in ΔH and ΔS, especially comparing to the significant range of ΔH and ΔS values (–145 to

21 kJ mol^{-1}, –621 to 44 J mol^{-1} K^{-1} respectively). The lack of strong convergence to an isoequilibrium when extrapolating from Figure 2 (also more clearly demonstrated in Figure S2) shows that this system however does not readily appear to meet the definitions to be an isokinetic relation (IKR).

This correlation between ΔS and ΔH can further be explored under the constraints that Sharp (2001) places on EEC for 95% confidence. The range of ΔG in this experiment is from –9 to 24.4 kJ mol^{-1} while the range of temperatures experiments were run was between –20 and –40 °C, (the harmonic mean being –30.3 °C or 242.9 K). While $|\Delta G| < |\Delta H|$ for most cases here, there is a significant range of $|\Delta G|$ and in the same magnitude as $|\Delta H|$ such that ΔG cannot be considered constant. The compensation temperature (235.5 K) however does fall within the 2σ range of the experimental temperature (242.9 K) and so this analysis alone does not meet the 95% confidence interval for nontrivial correlation. But, if the data from Fries et al. (2007) is included in this analysis, Tc and r^2 are instead 225.9 K and 0.9788 respectively with the harmonic mean experimental temperature as 244.9 K; this places Tc outside of the 2σ range of the experimental temperature and thus meets Sharp's criteria for a nontrivial correlation.

In regards to IKR as viewed through the Griessen et al. (2020) and Griessen and Dam (2021) EEC analysis, the Compensation Quality Factor (CQF) values are rather low, both below 0.25. This supports the observation of the absence of strong coalescence to an isoequilbrium and no noticeable IKR. The increase in CQF when including the data from Fries et al. (2007) also indicates that with the inclusion of more data, coalescence could be statistically inferred.

It should be noted that the explanation of EEC from solvation effects is not specific to aqueous systems. Computational work has identified instead two causes for EEC in solvent-solute interactions: solvent reorganization and molar shift (Grunwald and Steel, 1995). Regardless of aqueous nonspecificity, the EEC's implication of a surface liquid layer can still be made. There are other less likely potential explanations currently in literature such as the influence of hidden Carnot cycles from microphase transitions (Starikov and Nordén, 2007) or the loss of translational and rotational entropy during gas

phase association (Ryde, 2014). However, these seem unlikely to be the dominant mechanism for the EEC seen here and are outside the scope of discussion here.

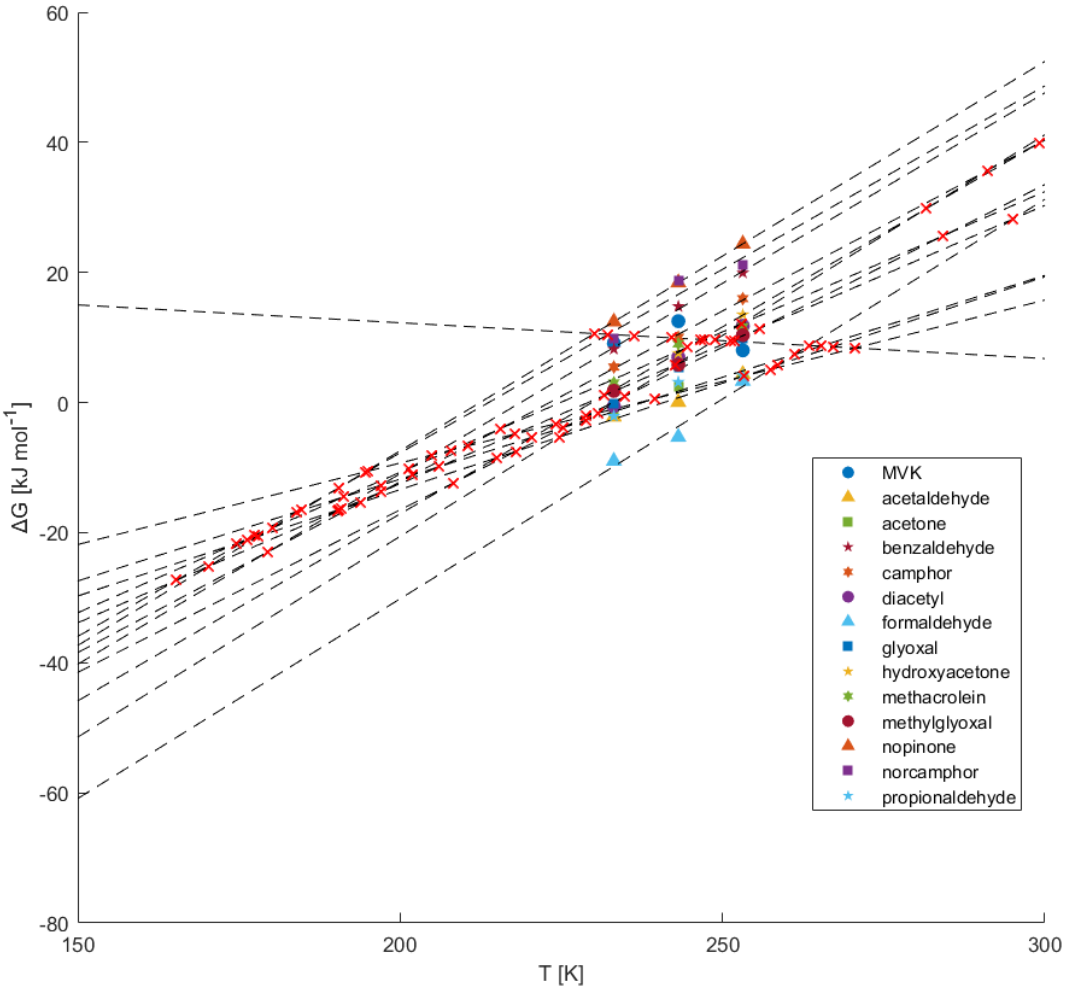

Figure S2. Plot of Temperature versus ΔG. Red x's indicate intersections of the extrapolated linear regressions.

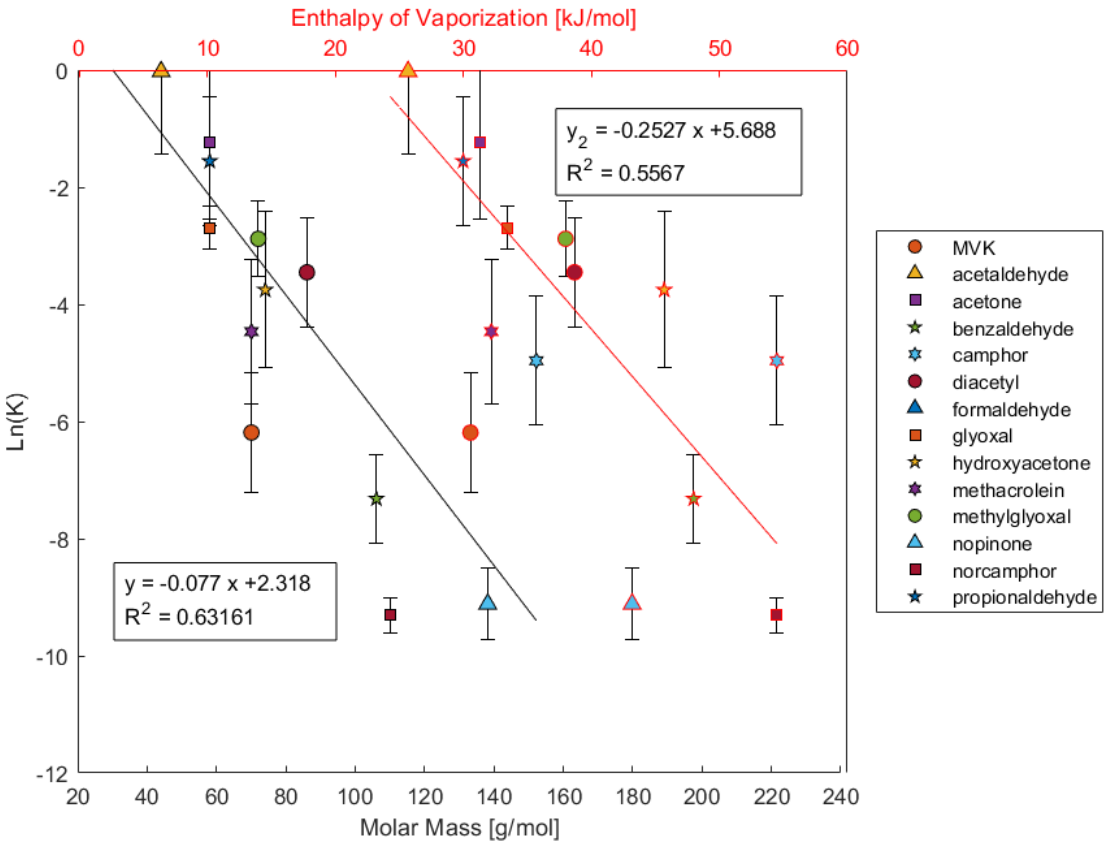

Figure S3. Scatterplot of ln(K) at –30 ºC versus the heat of vaporization (red line) and molar mass (black line).

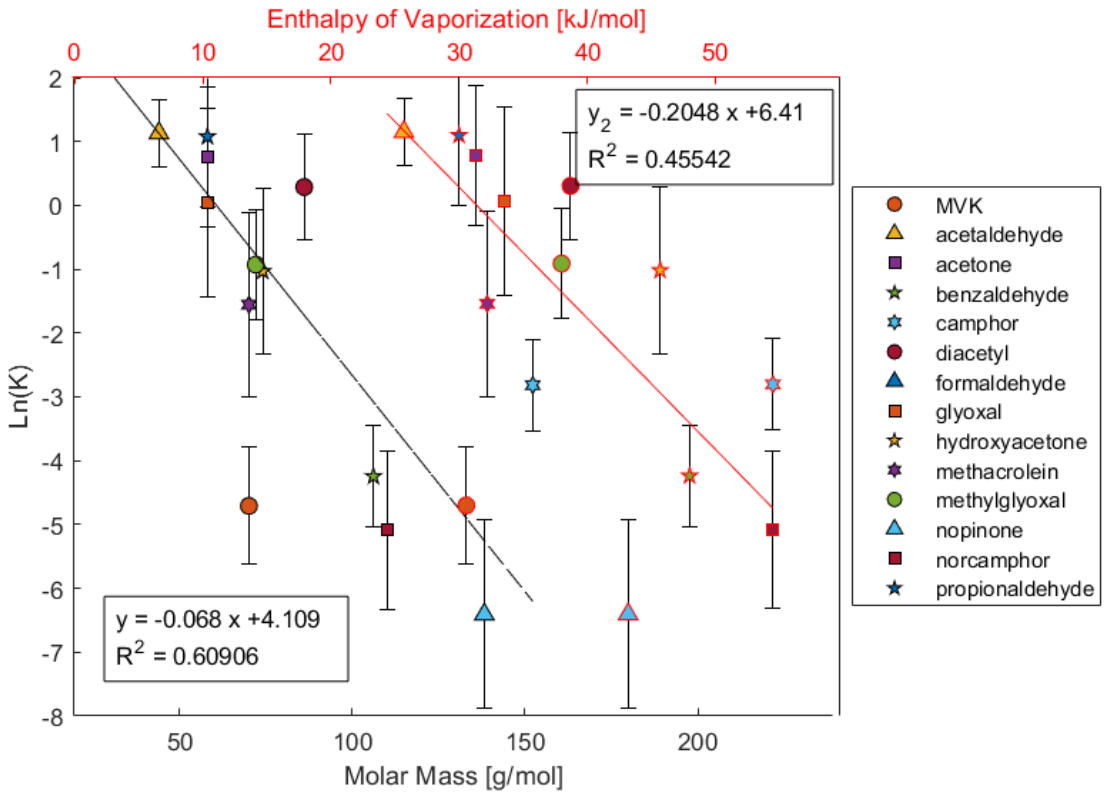

Figure S4. Scatterplot of ln(K) at –40 ºC versus the heat of vaporization (red line) and molar mass (black line).

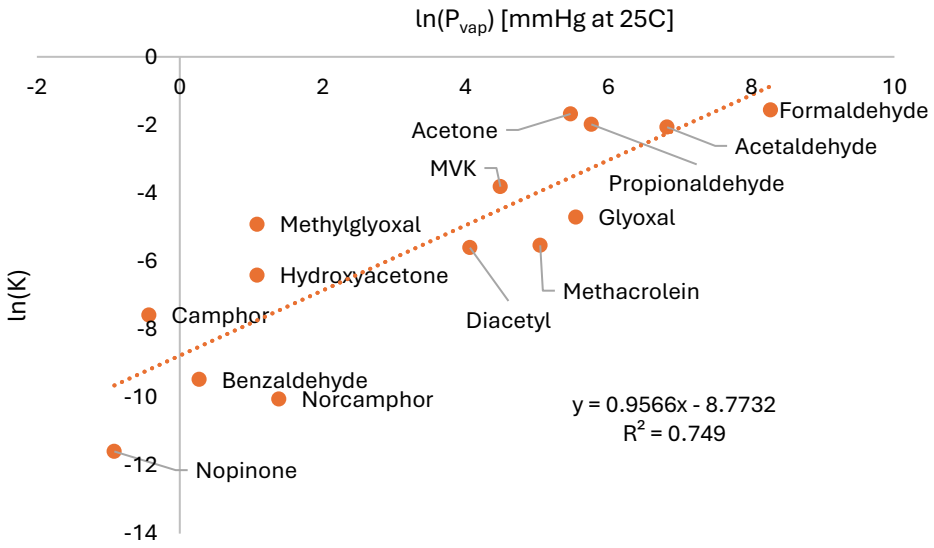

Figure S5. Scatterplot of ln(K) at –20 ºC versus the natural log of vapor pressure at 25 ºC.

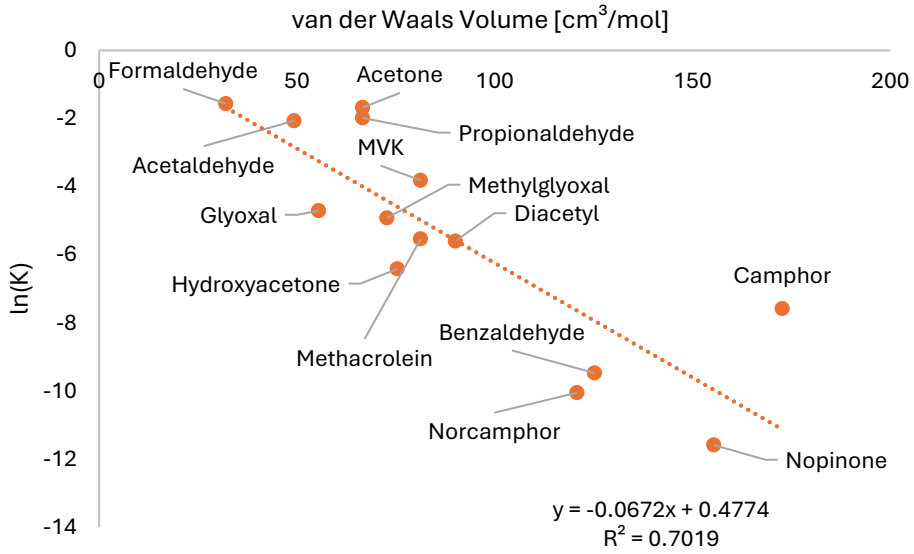

Figure S6. Scatterplot of ln(K) at –20 ºC versus the calculated van der Waals volume.

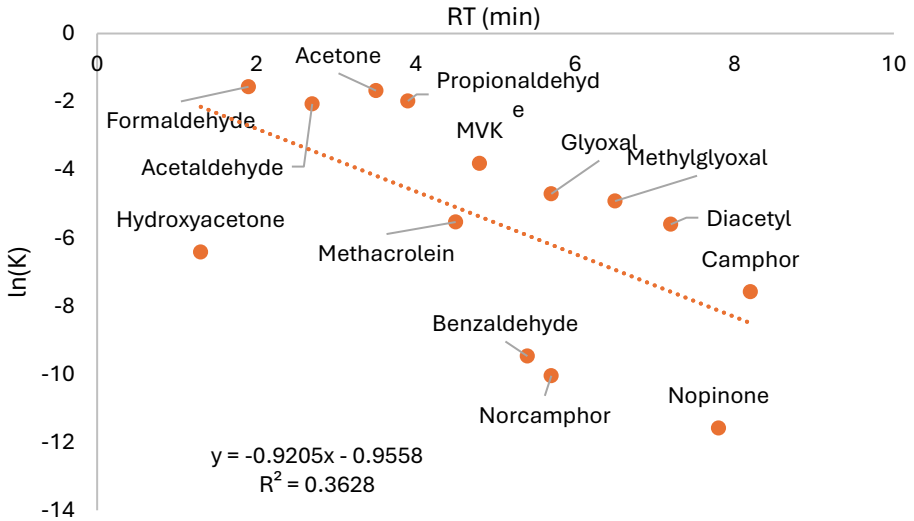

Figure S7. Scatterplot of ln(K) at –20 ºC versus the HPLC Retention Time (RT).

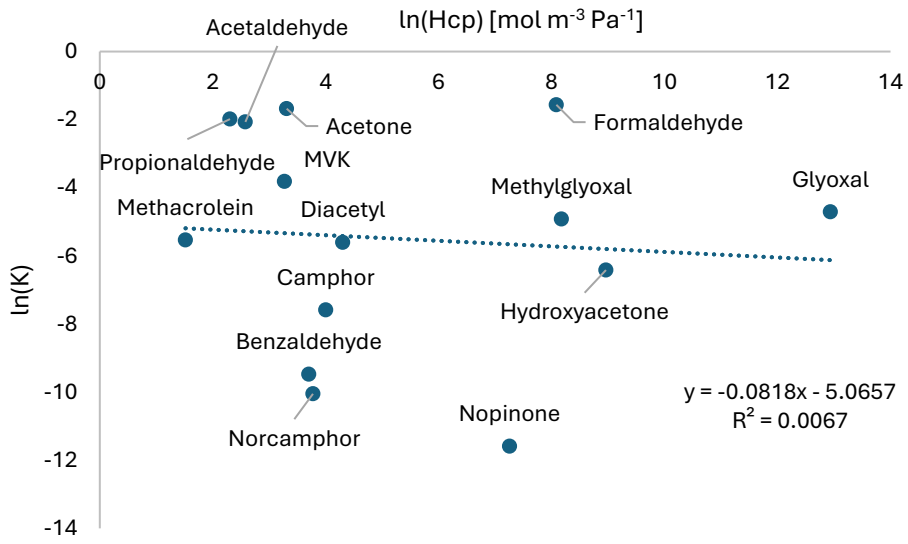

Figure S8. Scatterplot of ln(K) at –20 ºC versus the natural log of Henry solubility.

References

Fries, E., Starokozhev, E., Haunold, W., Jaeschke, W., Mitra, S. K., Borrmann, S., and Schmidt, M. U.: Laboratory studies on the uptake of aromatic hydrocarbons by ice crystals during vapor depositional crystal growth, Atmos Environ, 41, 6156–6166, https://doi.org/10.1016/j.atmosenv.2007.04.028, 2007.

Griessen, R. and Dam, B.: Simple Accurate Verification of Enthalpy-Entropy Compensation and Isoequilibrium Relationship, ChemPhysChem, 22, 1774–1784, https://doi.org/10.1002/CPHC.202100431, 2021.

Griessen, R., Boelsma, C., Schreuders, H., Broedersz, C. P., Gremaud, R., and Dam, B.: Single Quality Factor for Enthalpy-Entropy Compensation, Isoequilibrium and Isokinetic Relationships, ChemPhysChem, 21, 1632–1643, https://doi.org/10.1002/CPHC.202000390, 2020.

Grunwald, E. and Steel, C.: Solvent Reorganization and Thermodynamic Enthalpy-Entropy Compensation, J. Am. Chem. Soc, 5687–5692 pp., 1995.

Liu, L. and Guo, Q. X.: Isokinetic relationship, isoequilibrium relationship, and enthalpy-entropy compensation, https://doi.org/10.1021/cr990416z, March 2001.

Pan, A., Biswas, T., Rakshit, A. K., and Moulik, S. P.: Enthalpy-Entropy Compensation (EEC) Effect: A Revisit, Journal of Physical Chemistry B, 119, 15876–15884, https://doi.org/10.1021/acs.jpcb.5b09925, 2015.

Ryde, U.: A fundamental view of enthalpy-entropy compensation, Medchemcomm, 5, 1324–1336, https://doi.org/10.1039/c4md00057a, 2014.

Sharp, K.: Entropy—enthalpy compensation: Fact or artifact?, Protein Science, 10, 661–667, https://doi.org/10.1110/ps.37801, 2001.

Starikov, E. B. and Nordén, B.: Enthalpy-entropy compensation: A phantom or something useful?, Journal of Physical Chemistry B, 111, 14431–14435, https://doi.org/10.1021/JP075784I/ASSET/IMAGES/LARGE/JP075784IF00001.JPEG, 2007.